The AAPS Journal (2019) 21: 1
DOI: 10.1208/s12248-018-0272-z

Research Article

Theme: Pioneering Pharmaceutical Science by Emerging Investigators
Guest Editor: Ho-Leung Fung

Population Pharmacokinetics of AL-335 and Its Two Main Metabolites (ALS-022399, ALS-022227) in Monotherapy and in Combination with Odalasvir and/or Simeprevir

Elodie Valade,[1] Thomas N. Kakuda,[2] Matthew W. McClure,[2] Christopher Westland,[2] Belén Valenzuela,[3] Sivi Ouwerkerk-Mahadevan,[1] Juan José Perez-Ruixo,[1] and Oliver Ackaert[1,4]

Received 5 July 2018; accepted 9 October 2018; published online 24 October 2018

Abstract. The aim of the current study was to characterize the time course of plasma concentrations of AL-335 and its main metabolites (ALS-022399 and ALS-022227) after oral administration in healthy and hepatitis C virus (HCV)-infected subjects, in monotherapy as well as in combination with simeprevir and/or odalasvir. AL-335, ALS-022399, and ALS-022227 plasma concentrations from subjects receiving 800 mg of AL-335 orally once daily (qd) as monotherapy or in combination were pooled and analyzed using a nonlinear mixed effect modeling approach. The typical values (between subject variability) of AL-335 and ALS-022399 apparent linear clearances were 3300 L/h (33.9%) and 1910 L/h (30.0%), respectively. ALS-022227 elimination was characterized as a nonlinear process, with typical values of $V_{max,ALS\text{-}022227}$ and $K_{m,ALS\text{-}022227}$ estimated to be 84,799 ng/h (14.9%) and 450.2 ng/mL, respectively. AL-335 and ALS-022399 plasma concentrations were increased more than 2-fold in presence of simeprevir and/or odalasvir, while the effect on ALS-022227 plasma concentrations was limited. The effect of simeprevir and/or odalasvir might be explained by their capacity to inhibit P-glycoprotein. Internal evaluation confirmed that the population pharmacokinetic model developed was deemed appropriate to describe the time course of AL-335, ALS-022399, and ALS-022227 plasma concentrations and their associated variability in both healthy and HCV-infected subjects, as well as the interaction effect of simeprevir and/or odalasvir over AL-335 and its metabolites in healthy subjects. This model can be used as a starting point to evaluate drug-drug interaction processes in HCV-infected patients and support the development of a direct-acting antiviral (DAA) combination.

KEY WORDS: direct-acting antiviral (DAA) drugs; hepatitis C virus (HCV); nonlinear mixed effects modeling; pharmacokinetics; uridine nucleoside analog.

INTRODUCTION

Hepatitis C virus (HCV) infection is a disease with significant global impact. An estimated 71 million people worldwide are currently chronically infected with HCV that can lead to liver cirrhosis, hepatocellular carcinoma, liver failure, and liver failure-related death. Globally, chronic HCV infection and its complications account for 399,000 deaths every year (1).

The standard of care for hepatitis C infection has evolved quickly. Until 2011, treatment was based on interferon and ribavirin, and was associated with frequent and sometimes serious adverse reactions. Improvements in the understanding of the intracellular HCV life cycle (2) have allowed the identification of new targets and the development of direct-acting antivirals (DAAs). Interferon- and ribavirin-free combinations of DAAs are associated with high-sustained virologic response rates (> 95%) in chronic HCV-infected subjects and require shorter treatment duration (12 weeks or less) compared to previous therapies.

It is recommended to treat chronic HCV-infected subjects with at least 2 DAAs targeting different proteins involved in the HCV life cycle: the viral nonstructural (NS)

Guest Editor: Ho-Leung Fung

Matthew W. McClure Affiliation is currently Second Genome, South San Francisco, CA, USA

[1] Janssen Research and Development, Global Clinical Pharmacology, Turnhoutseweg 30, B-2340, Beerse, Belgium.
[2] Alios BioPharma, Inc., part of the Janssen Pharmaceutical Companies, South San Francisco, California, USA.
[3] SGS Exprimo NV, Mechelen, Belgium.
[4] To whom correspondence should be addressed. (e–mail: oackaert@ITS.JNJ.com)

3/4A protease, the NS5B polymerase, and/or the NS5A protein (3). Data from several clinical trials have demonstrated the potential for the effective combination of a nucleotide analogue NS5B polymerase inhibitor with NS3/4A protease or NS5A inhibitors for the treatment of chronic HCV infection (4,5). Available data also suggest that adding a third anti-HCV agent may increase the robustness of the regimen, allowing for a shorter treatment duration while maintaining a high efficacy (5). The prodrug AL-335 is an investigational HCV nonstructural protein (NS)5B inhibitor (6). In vivo, AL-335 is rapidly converted to ALS-022399 (monophosphate precursor) by cathepsin A and carboxylesterase, then subsequently phosphorylated intracellularly (data on file) to the triphosphate ALS-022235. The active moiety of AL-335, ALS-022235 (5′-triphosphate), inhibits HCV NS5B ribonucleic acid (RNA)-dependent RNA polymerase by acting as a chain terminator of RNA synthesis (7). Dephosphorylation of ALS-022235 yields the parent nucleoside ALS-022227. Nucleoside polymerase inhibitors have demonstrated their potential to provide a high barrier to the development of resistance, antiviral activity against multiple HCV genotypes, and favorable clinical safety profile (8). AL-335 was investigated in combination with odalasvir, an NS5A inhibitor, and simeprevir, an approved NS3/4A protease inhibitor for the treatment of chronic HCV infection (9).

The pharmacokinetics of AL-335 and its two metabolites has been previously characterized in two clinical studies, AL-335-601 (NCT02339207) (McClure MW, Berliba E, Tsertsvadze T, Streinu-Cercel A, Vijgen L, Astruc B, *et al.* Safety, tolerability and pharmacokinetics of AL-335 in healthy volunteers and hepatitis C virus-infected subjects, manuscript under review) and AL-335-602 (NCT02512562) (10). AL-335-601 evaluated the pharmacokinetics of AL-335 and its metabolites after single- and multiple-ascending dose in healthy subjects and as monotherapy in HCV-infected subjects. The pharmacokinetic profile of AL-335 in healthy volunteers or HCV-infected subjects showed that the prodrug AL-335 was rapidly absorbed and converted to ALS-022399 and ALS-022227, as indicated by the short half-life of AL-335 (mean $t_{1/2} \leq 1$ h for all doses) and the quick appearance of ALS-022399 and ALS-022227. Exposure to AL-335 increased in a dose-proportional and less than dose-proportional manner in HCV-infected subjects and healthy volunteers, respectively. Exposure to ALS-022399 increased in a dose-proportional manner both in healthy volunteers and HCV-infected subjects whereas exposure to ALS-022227 increased in a less than dose-proportional manner both in healthy volunteers and HCV-infected subjects. (McClure MW, Berliba E, Tsertsvadze T, Streinu-Cercel A, Vijgen L, Astruc B, *et al.* Safety, tolerability and pharmacokinetics of AL-335 in healthy volunteers and hepatitis C virus-infected subjects, manuscript under review). AL-335-602 was designed to evaluate the safety and pharmacokinetics of AL-335 and its main metabolites, when administered alone or in combination with simeprevir and/or odalasvir, in healthy subjects. Odalasvir has been reported to be a P-glycoprotein inhibitor (10), simeprevir a P-glycoprotein substrate and inhibitor (11), and AL-335 a P-glycoprotein substrate (10). Understanding the pharmacokinetic behavior of AL-335 and its two main metabolites given in combination with simeprevir and/or odalasvir and assessing the drug-drug interactions was critical for the dose selection and the development of this 3 DAA combination.

Therefore, the objectives of this analysis were to characterize the pharmacokinetics of AL-335 and its two main metabolites (ALS-022399 and ALS-022227) in monotherapy in healthy and chronically HCV-infected subjects, as well as to quantify the interaction of simeprevir and/or odalasvir on the pharmacokinetics of AL-335, ALS-022399, and ALS-022227 in healthy subjects.

MATERIALS AND METHODS

Subject Eligibility Criteria and Clinical Data

The study population included healthy and HCV-infected subjects without cirrhosis from the clinical studies, AL-335-601 (McClure MW, Berliba E, Tsertsvadze T, Streinu-Cercel A, Vijgen L, Astruc B, *et al.* Safety, tolerability and pharmacokinetics of AL-335 in healthy volunteers and hepatitis C virus-infected subjects, manuscript under review) and AL-335-602 (10). Each protocol was reviewed and approved by an institutional review board and written informed consent was obtained from each subject before enrollment in the studies, after being advised of the potential risks and benefits of the study. The studies were conducted in agreement with the Declaration of Helsinki, Good Clinical Practices guidelines, and other applicable regulatory requirements.

Table I provides a summary of the studies' characteristics and available data. Healthy and HCV-infected subjects received multiple doses of 800 mg AL-335 orally once a day (qd) with a standard meal. Other dose levels and food conditions were investigated in study AL-335-601 but were not included in the current analysis as the dose of 800 mg qd in fed conditions was selected for further clinical development. In the drug-drug interaction study AL-335-602, subjects in treatment group 1 received 800 mg AL-335 qd on days 1–3, 11–13, and 21–23; 150 mg of simeprevir qd on days 4–23 and a 150 mg loading dose of odalasvir on day 14 followed by 50 mg odalasvir qd on days 15–23 with standard meals. Subjects in treatment group 2 received 800 mg AL-335 qd on days 1–3, 11–13, and 21–23; a 150 mg loading dose of odalasvir on day 4 followed by 50 mg odalasvir qd on days 5–23 and 150 mg of simeprevir qd on days 14–23 with standard meals. A study schematic of AL-335-602 is available Fig. 1.

Plasma PK samples were collected at specified times for each study as detailed in Table I and were analyzed using validated liquid chromatography with tandem mass spectrometry method. The lower limit of quantification (LLOQ) was 1 ng/mL, 2 ng/mL, and 5 ng/mL for AL-335, ALS-022399, and ALS-022227, respectively. Concentrations were transformed to micromoles per liter of the parent drug and its metabolites, to avoid stoichiometry issues during the population pharmacokinetic analysis.

Pharmacokinetic Model Development

Software. The data were analyzed by a nonlinear mixed effects modeling approach using NONMEM software (version 7.3; Icon Development Solutions, Ellicot City, MD,

Table I. Summary of the Studies and Available Data Included in the Analysis

Item	AL-335-602 study (10)	AL-335-601 study
Study (population)	Healthy subjects	Chronic HCV-infected subjects
No. of subjects	31	27
Treatments	800 mg AL-335 monotherapy ($n = 31$) 800 mg AL-335 + 150 mg SMV ($n = 15$) 800 mg AL-335 + 50 mg ODV ($n = 15$) 800 mg AL-335 + 150 mg SMV + 50 mg ODV ($n = 29$)	800 mg AL-335 monotherapy
Dosing frequency	qd	qd
PK sampling schedule	At pre-dose, 0.25, 0.5, 1, 2, 3, 4, 6, 8, 10, 12, and 24 h post-doseOn day 3 (monotherapy), day 13 (SMV + AL-335 or ODV + AL-335), and day 23 (SMV + ODV + AL-335)	Day 1: pre-dose, 0.25, 0.5, 1, 2, 3, 4, 6, 8, 12 h post-dose Day 2 to 6: pre-dose Day 7: pre-dose, 0.25, 0.5, 1, 2, 3, 4, 6, 8, 12, 24, 36, 48, 72, 96, 120 h post-dose Day 21
No. conc. (BLQ)		
AL-335	687 (127)	370 (59)
ALS-022399	818 (197)	428 (244)
ALS-022227	1079 (1)	712 (69)

Time points where concentrations were BLQ for all subjects were not counted as BLQ in this analysis
Conc. plasma concentrations, *ODV* odalasvir, *qd* once daily, *SMV* simeprevir

USA) (12). The first-order conditional estimation (FOCE) method was used for the analysis. Dataset preparation, exploration, visualization, and graphical analysis of NONMEM outputs were conducted using R (version 3.3.2; R Development Core Team, Vienna, Austria) (13).

Structural Model. A stepwise approach was used for the model building: first, a model describing the pharmacokinetics of AL-335, ALS-022399, and ALS-022227 in monotherapy was developed, after which the interaction of simeprevir and/or odalasvir on the pharmacokinetics of AL-335, ALS-022399, or ALS-022227 was quantified. For the development of the monotherapy model, a sequential approach was selected to account for the greater number of observations of ALS-022227 relative to ALS-022399 or AL-335. Structural models for ALS-022399 and ALS-022227 were selected with parameters of the previous entities being fixed. Once the structural model was identified for each of the three compounds, a joint population pharmacokinetic model for AL-335 and its two metabolites was fitted to the whole data. Different absorption models, such as zero- or first-order absorption processes, parallel first-order absorption, parallel first- and zero-order absorption, and sequential zero- and first-order absorption were investigated to describe the absorption of AL-335. The presence of a lag time in the drug absorption process was also explored. In addition, disposition models with different number of compartments as well as with linear and nonlinear elimination processes were explored to describe the disposition of AL-335, ALS-022399, and ALS-022227. The absence of parent drug and metabolites data after intravenous administration did not allow quantification of either the bioavailability of the parent drug or the fraction of parent drug transformed into the first metabolite and, subsequently, the fraction of first metabolite transformed into the second metabolite. Therefore, in this analysis, the fraction absorbed of AL-335 was assumed to be 1 and the disposition parameter estimates for AL-335, ALS-022399, and ALS-022227 were apparent (14). It was also assumed that

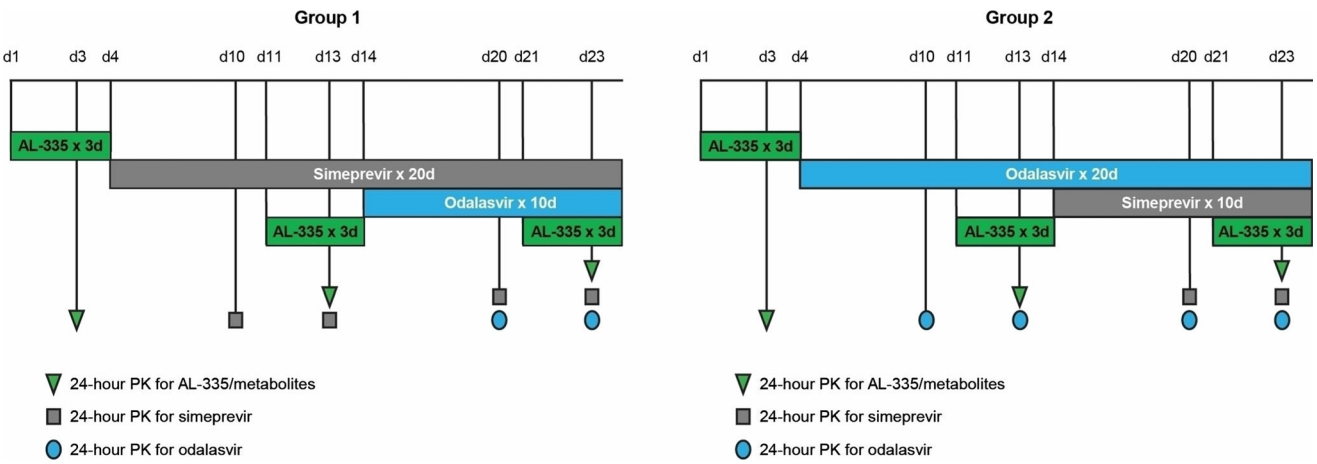

Fig. 1. Schematic of the clinical study design for AL-335-602 study (treatments and sampling schedule). Green triangles represent blood sampling for AL-335; gray squares represent blood sampling for simeprevir, and blue circles represent blood sampling for odalasvir

AL-335 was completely converted into ALS-022399, and that ALS-022399 was completely transformed into ALS-022227.

The effect of simeprevir, odalasvir, or simeprevir + odalasvir was evaluated separately on different pharmacokinetic parameters (P) as a categorical effect and was implemented as follows:

$$P = \theta_P \times \theta_{SMV}{}^{SMV} \times \theta_{ODV}{}^{ODV} \times \theta_{SMV+ODV}{}^{SMV+ODV} \quad (1)$$

where θ_P is the pharmacokinetic parameter estimate without co-administration of simeprevir, odalasvir or simeprevir + odalasvir. θ_{SMV}, θ_{ODV}, and $\theta_{SMV+ODV}$ accounted for the change in θ_P in presence of simeprevir, odalasvir, or both (simeprevir + odalasvir), as a significant dual interaction between simeprevir and odalasvir has been previously reported and quantified using a population pharmacokinetic modeling approach (15). The impact of demographic covariates such as age, gender, and body weight on the exposure of AL-335 and its metabolites was not evaluated in this analysis.

Statistical Model. The interindividual (or between subjects) variability (IIV) in the pharmacokinetic model parameters was assumed to follow a log-normal distribution and, consequently, an exponential error model was used. Residual variability in AL-335, ALS-022399, and ALS-022227 was separately evaluated using an additive error model after natural logarithmic transformation of the observations and model predictions.

Model Selection Criteria. To discriminate hierarchical models, the log-likelihood ratio test was used. A decrease of the objective function value (OFV) of more than 6.63 points (theoretically coinciding with a p value < 0.01, assuming one degree of freedom (df)) was considered as a significant improvement. Akaike information criterion (AIC) and Bayesian information criterion (BIC) were used to discriminate non-embedded models. The effect of simeprevir and/or odalasvir over the pharmacokinetic parameters of the three entities was included in the model when the OFV decrease was statistically significant ($\Delta OFV > -6.63$, $df = 1$, $p < 0.01$). In parallel to this statistical method, a graphical evaluation of the goodness of fit was performed by plotting the observed concentrations versus population predictions (PRED) or individual predictions (IPRED), conditional weighted residuals (CWRES) versus time, and CWRES versus PRED. A successful minimization process with a non-aborted covariance step, as well as relative standard error (RSE) $< 50\%$ were also considered to discriminate between models.

Model Qualification. Two complementary methods were employed to evaluate the model developed: normalized prediction distribution errors (NPDE) (16,17), and visual predictive check (VPC) (18). The distribution of the NPDE was explored by a scatterplot of NPDE versus the population prediction and time. The VPC display the 5th, 50th, and 95th percentiles of the observed values, and the 95% confidence interval (CI) for the corresponding model-based predicted percentiles computed from 500 Monte Carlo replicates obtained by simulating the design of the underlying dataset with the final model parameters.

Model-Based Simulations. Based on the pharmacokinetic model developed, deterministic simulations were performed to explore the time course of AL-335, ALS-022399, and ALS-022227 plasma concentrations at steady-state after a daily dose administration of 800 mg under monotherapy regimen and in combination with the following: (a) 150 mg of simeprevir orally qd, (b) 50 mg of odalasvir orally qd, or (c) 150 mg of simeprevir + 50 mg of odalasvir orally qd.

RESULTS

A total of 58 subjects (31 healthy subjects and 27 HCV-infected subjects) were included in the analysis. The population pharmacokinetic analysis was developed with a total of 4094 plasma concentrations (1057 from AL-335, 1246 from ALS-022399, and 1791 from ALS-022227). A total of 14.96%, 26.14%, and 3.76% plasma concentrations for AL-335, ALS-022399, and ALS-022227, respectively, were below LLOQ data and were excluded from the analysis.

A schematic of the pharmacokinetic model used to describe the time course of the parent drug and its metabolites after oral administration is displayed in Fig. 2. AL-335 absorption process was well characterized by a sequential zero- and first-order absorption processes, parametrized in terms of the duration of the zero-order absorption process (D1) and the first-order absorption rate constant (ka), after a lag time period before the zero-order process (ALAG). An open one-compartment disposition model parameterized in terms of apparent central volume of distribution ($V_{AL\text{-}335}$) and linear clearance ($CL_{AL\text{-}335}$) was suitable to describe AL-335 pharmacokinetics. The pharmacokinetics of ALS-022399 was described using an open two-compartment disposition model with linear elimination. The model was parametrized in terms of central volume of distribution ($V_{ALS\text{-}022399}$), linear clearance from central compartment ($CL_{ALS\text{-}022399}$), intercompartmental flow between central and peripheral compartment ($Q_{ALS\text{-}022399}$), and volume of distribution of peripheral compartment ($V_{p,ALS\text{-}022399}$). Finally, for ALS-022227, an open two-compartment disposition model with nonlinear elimination from the central compartment was used. The model was parametrized in terms of central volume of distribution ($V_{ALS\text{-}022227}$), nonlinear clearance from central compartment described by the maximum velocity of the elimination ($V_{max,ALS\text{-}022227}$) and the Michealis-Menten constant ($K_{m,ALS\text{-}022227}$), intercompartmental flow between central and peripheral compartment ($Q_{ALS\text{-}022227}$), and volume of distribution of peripheral compartment ($V_{p,ALS\text{-}022227}$). The equations describing the time course of AL-335, ALS-022399, and ALS-022227 were as follows:

$$\text{If } t < \text{ALAG}, \text{then } \frac{dA_1}{dt} = 0$$

$$\text{If } t \geq \text{ALAG}, \text{then } \frac{dA_1}{dt} = k_0 - k_a \cdot A_1 \text{ where } k_0$$

$$= \text{Dose/D1 in the time interval between} \quad (2)$$

$$\text{t} = \text{ALAG and t} = \text{ALAG} + \text{D1}, \text{and 0 otherwise}$$

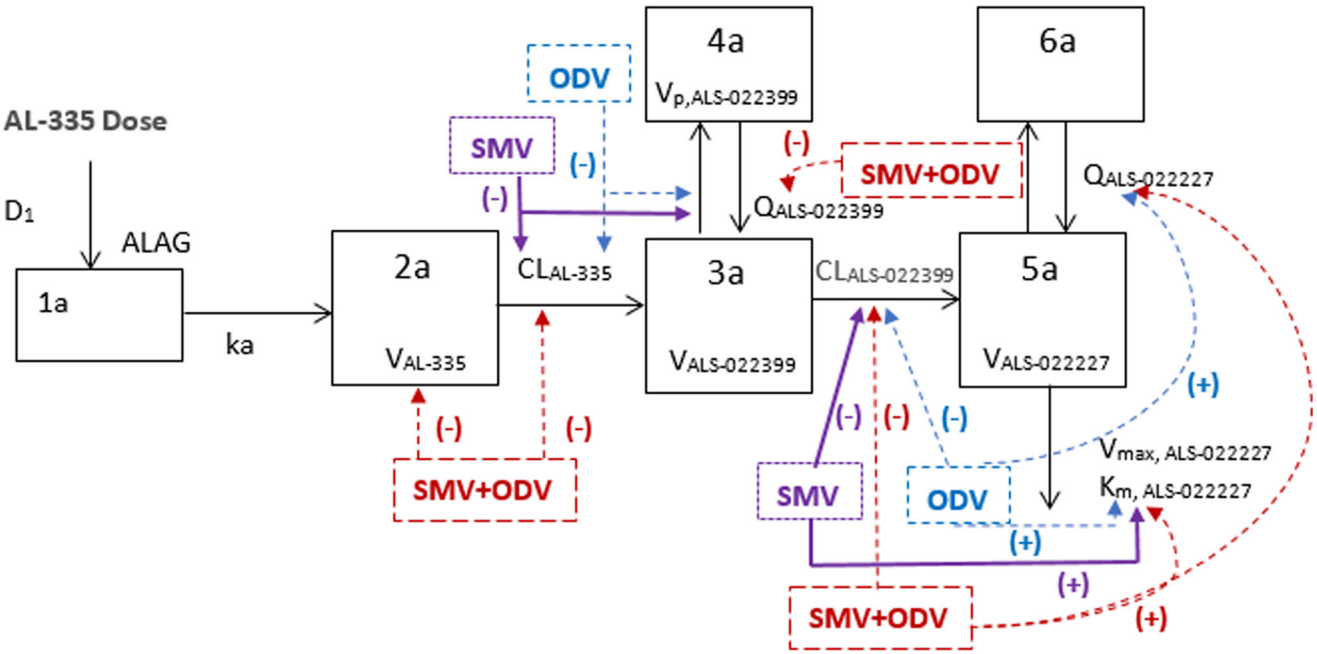

Fig. 2. Schematic of the population pharmacokinetic model for AL-335, ALS-022399, and ALS-022227. (−) and (+) indicates a reduction or an increase on the pharmacokinetic parameter value in presence of simeprevir (SMV) and/or odalasvir (ODV)

$$\frac{dA_2}{dt} = k_a \cdot A_1 - \frac{CL_{AL-335}}{V_{AL-335}} \cdot A_2 \tag{3}$$

$$\frac{dA_3}{dt} = \frac{CL_{AL-335}}{V_{AL-335}} \cdot A_2 - \frac{Q_{ALS-022399}}{V_{ALS-022399}} \cdot A_3 + \frac{Q_{ALS-022399}}{V_{p,ALS-022399}} \cdot A_4 - \frac{CL_{ALS-022399}}{V_{ALS-022399}} \cdot A_3 \tag{4}$$

$$\frac{dA_4}{dt} = \frac{Q_{ALS-022399}}{V_{ALS-022399}} \cdot A_3 - \frac{Q_{ALS-022399}}{V_{p,ALS-022399}} \cdot A_4 \tag{5}$$

$$\frac{dA_5}{dt} = \frac{CL_{ALS-022399}}{V_{ALS-022399}} \cdot A_3 - \frac{Q_{ALS-022227}}{V_{ALS-022227}} \cdot A_5 + \frac{Q_{ALS-022227}}{V_{p,ALS-022227}} \cdot A_6 - \frac{V_{max,ALS-022227}}{(K_{m,ALS-022227} + A_{5/V_{ALS-022227}})} \cdot A_5 / V_{ALS-022227} \tag{6}$$

$$\frac{dA_6}{dt} = \frac{Q_{ALS-022227}}{V_{ALS-022227}} \cdot A_5 - \frac{Q_{ALS-022227}}{V_{p,ALS-022227}} \cdot A_6 \tag{7}$$

where A_1 and A_2 represent the AL-335 amounts in depot and central compartment, respectively. A_3 and A_4 represent the amounts of ALS-022399 in central and peripheral compartment, respectively, while A_5 and A_6 represent the amounts of ALS-022227 in central and peripheral compartment, respectively. The rest of terms have been previously defined in the text.

For AL-335, more complex disposition pharmacokinetic models (e.g., two-compartment model) did not significantly improve the model fit. Simplification in the model considering only a first-order absorption process was not able to correctly describe the absorption process (ΔMVOF = 47.92 points). In this structural model, IIV was estimated for CL_{AL-335}, V_{AL-335}, D1, and ALAG. The estimation of IIV on ka did not evidence any significant improvement in the model fit and, consequently, was set to 0.

For ALS-022399, an open two-compartment linear model was significantly better than a one-compartment model to characterize the disposition of ALS-022399 (ΔMVOF = 208.73 points). IIV was estimated on $CL_{ALS-022399}$ and $V_{ALS-022399}$. Attempts to quantify the IIV on $Q_{ALS-022399}$ and $V_{p,ALS-022399}$ did not improve the model. Finally, an open two-compartment model with nonlinear elimination was significantly better to describe the temporary evolution of ALS-022227 plasma concentrations than a one-compartment model with linear or nonlinear elimination. For ALS-022227, IIV was quantified on $V_{max,ALS-022227}$ and $V_{ALS-022227}$.

The developed model was applied to patient data following administration of AL-335 in monotherapy and potential differences in pharmacokinetics between healthy and chronic HCV-infected subjects were evaluated for each PK parameter. Based on the current analysis D1 was 46% higher in HCV-infected subjects compared to healthy subjects; however, the underlying physiological process responsible of this empirical finding remains unknown. Estimation of one absorption lag time for both populations resulted in high RSE for this parameter. The estimation of a specific absorption lag time for chronic HCV-infected subjects was

very small and with high RSE. Therefore, no lag time for chronic HCV-infected subjects was considered in the model. No other statistical differences in absorption or disposition parameters were found between healthy subjects and HCV-infected subjects.

The final model parameter estimates and their associated precisions, measured as RSE, are presented in Table II. Fixed effects were estimated with good precision (RSE <25%), while the precision in the estimate of random effect was reasonable. The shrinkage in random effects was, in general, acceptable (see Table II), except for ALAG (42.3%).

The interaction model revealed that $CL_{AL\text{-}335}$ was reduced by 62.9%, 68.8%, and 86.6% in presence of odalasvir, simeprevir, or simeprevir + odalasvir, respectively. $CL_{ALS\text{-}022399}$ was also reduced when co-administered but to a lower extent (51.0%, 33.9%, and 60.2%, respectively). In contrast, the effect of simeprevir and odalasvir over ALS-022227 increased the values of $K_{m,ALS\text{-}022227}$ by 21% and 44%, respectively, and by 55% in presence of simeprevir + odalasvir. The inclusion of an effect of odalasvir + simeprevir on AL-335 relative bioavailability instead of two different effects on $CL_{AL\text{-}335}$ and $V_{AL\text{-}335}$ was also tested but gave a higher OFV. As the effect of odalasvir + simeprevir on $CL_{AL\text{-}335}$ was clearly the most significant, the addition of an effect on AL-335 bioavailability on top of the effect on $CL_{AL\text{-}335}$ was investigated but led to model instability. Simeprevir and/or odalasvir significantly affected other pharmacokinetic parameters as shown in Table II.

Table II. AL-335, ALS-022399, and ALS-022227 Population Pharmacokinetic Parameters in Monotherapy and in Combination with Odalasvir and/or Simeprevir

Parameter (unit)	Typical value[a] (RSE, %)	Between subjects variability[b] (RSE, %)
AL-335		
ALAG[c] (h)	0.0812 (19.0)	61.4 (51.7)
D_1 (h)	1.67 (9.3)	45.9 (24.6)
$D_{1\_HCV\ infected\ subjects}$ (h)	2.43 (14.4)	45.9 (24.6)
k_a (h^{-1})	0.958 (2.6)	
$V_{AL\text{-}335}$/F (L)	697 (14.6)	80.9 (27.5)
Effect of SMV + ODV on $V_{AL\text{-}335}$/F	0.350 (22.2)	
$CL_{AL\text{-}335}$/F (L/h)	3300 (5.3)	33.9 (21.5)
Effect of SMV on $CL_{AL\text{-}335}$/F	0.312 (9.7)	
Effect of ODV on $CL_{AL\text{-}335}$/F	0.371 (10.4)	
Effect of SMV + ODV on $CL_{AL\text{-}335}$/F	0.134 (9.5)	
$\sigma_{AL\text{-}335}$	73.9 (4.1)	
ALS-022399		
$V_{ALS\text{-}022399}$/F (L)	1620 (7.5)	31.9 (47.9)
$CL_{ALS\text{-}022399}$/F (L/h)	1910 (3.9)	21.0 (20.1)
Effect of SMV on $CL_{ALS\text{-}022399}$/F	0.661 (7.2)	
Effect of ODV on $CL_{ALS\text{-}022399}$/F	0.490 (7.1)	
Effect of SMV + ODV on $CL_{ALS\text{-}022399}$/F	0.398 (6.6)	
$Q_{ALS\text{-}022399}$/F (L/h)	4840 (15.0)	
Effect of SMV on $Q_{ALS\text{-}022399}$/F	0.284 (27.5)	
Effect of ODV on $Q_{ALS\text{-}022399}$/F	0.0461 (26.7)	
Effect of SMV + ODV on $Q_{ALS\text{-}022399}$/F	0.0388 (24.9)	
$V_{p,ALS\text{-}022399}$/F (L)	5720 (11.6)	
$\sigma_{ALS\text{-}022399}$	43.7 (4.7)	
ALS-022227		
$V_{ALS\text{-}022227}$/F (L)	76.2 (13.0)	78.7 (28.4)
$V_{max,ALS\text{-}022227}$/F (μmol/h)[d]	307 (13.4)	14.9 (20.7)
$K_{m,ALS\text{-}022227}$ (μM)[d]	1.63 (19.8)	
Effect of SMV on $K_{m,ALS\text{-}022227}$	1.21 (4.8)	
Effect of ODV on $K_{m,ALS\text{-}022227}$	1.44 (6.7)	
Effect of SMV + ODV on $K_{m,ALS\text{-}022227}$	1.55 (7.1)	
$Q_{ALS\text{-}022227}$/F (L/h)	29.9 (12.7)	
Effect of ODV on $Q_{ALS\text{-}022227}$/F	3.2 (16.8)	
Effect of SMV + ODV on $Q_{ALS\text{-}022227}$/F	3.5 (13.1)	
$V_{p,ALS\text{-}022227}$/F (L)	981 (7.6)	
$\sigma_{ALS\text{-}022227}$	26.2 (3.7)	

The shrinkage values (%) for $CL_{AL\text{-}335}$/F, $V_{AL\text{-}335}$/F, D1, $CL_{ALS\text{-}022399}$/F, $V_{ALS\text{-}022399}$/F, $V_{max,\ ALS\text{-}022227}$/F, and $V_{ALS\text{-}022227}$/F were 11.4, 16.5, 5.2, 5.1, 29.2, 1.7, and 10.6, respectively

[a] Results expressed as parameter (*RSE* relative standard error of parameter estimate, %)

[b] Between subjects variability and residual variability (σ) expressed as coefficient of variation (%)

[c] No ALAG was determined in HCV-infected subjects

[d] Molar units were transformed to dosing units taking into account the molecular weight of ALS-022227 (276.2 g/mol)

Figures 3 and 4 show the goodness-of-fit plots of the final model. In Fig. 3, the scatter plots representing the observed plasma concentration vs the population (left panels) and individual (right panels) model predictions for the three compounds showed a normal random scatter around the identity line, indicating the absence of significant bias. Similarly, the distribution of CWRES (Fig. 4) as a function of the population predictions (left panels) and time (right panels) did not show any trend that evidences model inadequacy or misfit. For AL-335 and ALS-022399, a small deviation from the identity line can be observed at lower concentrations and at the later time points, which can be explained because of the observations below LLOQ for these two compounds. In addition, histograms of the individual Bayesian estimates of pharmacokinetic parameters exhibited centered distribution around the population typical value (data not shown).

The results of the VPC are showed in Figs. 5 and 6. These figures indicate that the model developed is appropriate to describe the time course of plasma concentrations of AL-335, ALS-022399, and ALS-022227, and their variability in both healthy and HCV-infected subjects, regardless the administration of the parent drug in monotherapy (Fig. 5) or in combination regimens including simeprevir and/or odalasvir (Fig. 6).

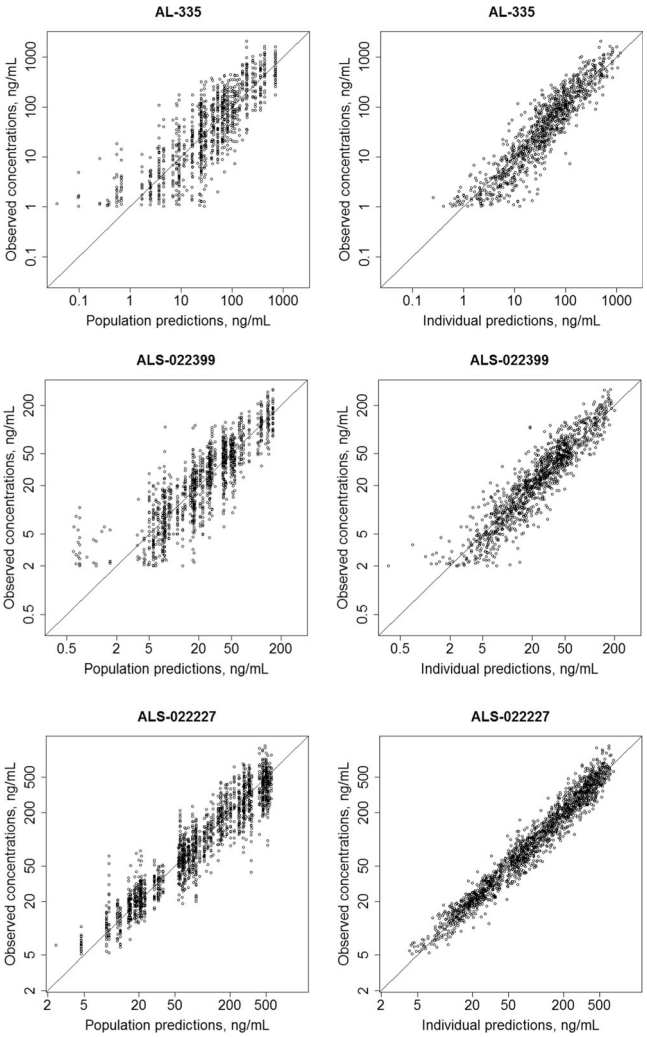

Fig. 3. Goodness of fit plots for AL-335, ALS-022399, and ALS-022227

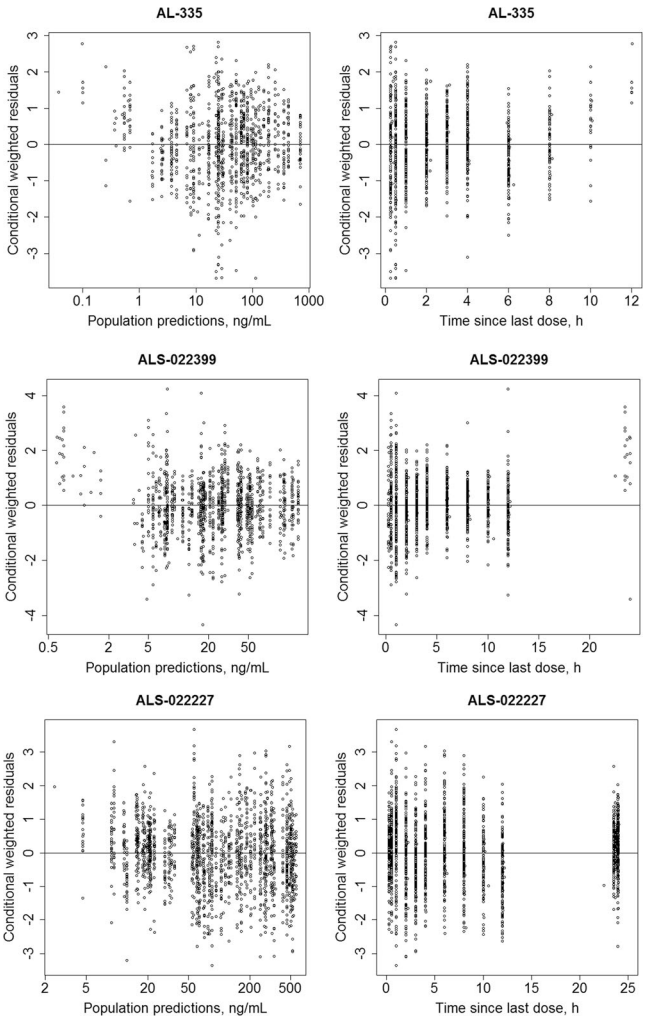

Fig. 4. Goodness of fit plots for AL-335, ALS-022399, and ALS-022227

In addition, the distribution of the NPDE as a function of the population predictions (Fig. 7, left panels) and time (Fig. 7, right panels) did not show any trend that evidenced model misfit, and confirmed the model accuracy and precision in describing plasma concentrations of AL-335, ALS-022399, and ALS-022227, and their variability in healthy and HCV-infected subjects following oral AL-335 administration in absence or presence of odalasvir and or simeprevir administration.

Deterministic simulations (Fig. 8) showed that AL-335 and ALS-022399 exposures are higher in presence of simeprevir or odalasvir and this effect is even more pronounced when both drugs are co-administered with AL-335. Additionally, ALS-022227 plasma concentrations are slightly higher in presence of simeprevir and/or odalasvir (mainly from 8 h after the drug administration) but the magnitude of the effect is much lower compared to AL-335 and ALS-022399 and probably not clinically relevant.

DISCUSSION

The main goal of this analysis was to characterize the plasma concentration time profiles of AL-335 and its two

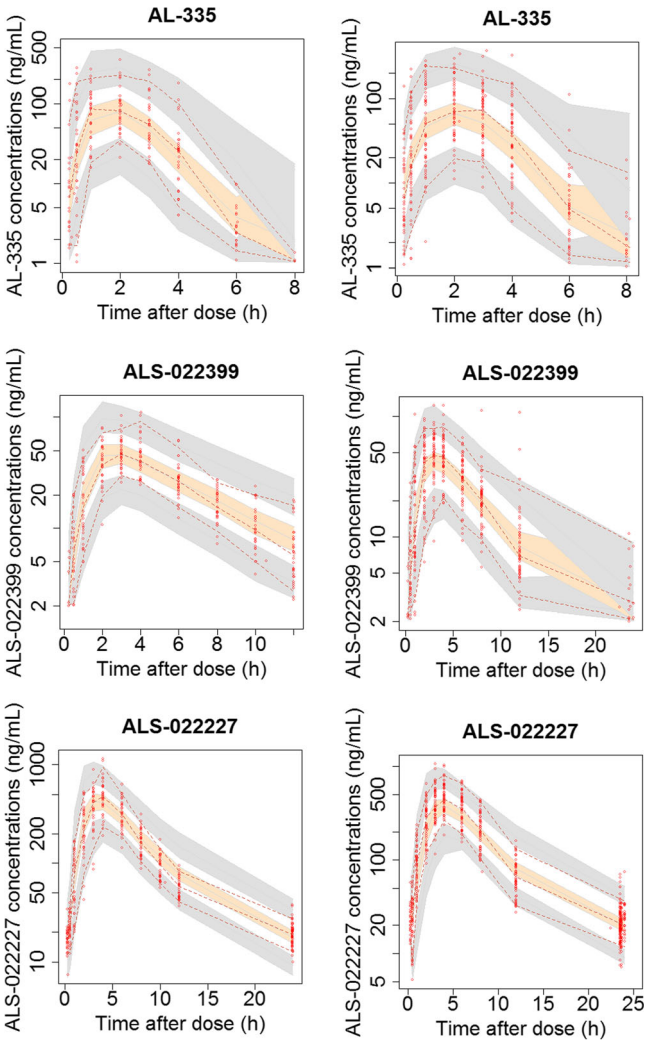

Fig. 5. Visual predictive check of AL-335, ALS-022399, and ALS-022227 in monotherapy for healthy subjects (left panels) and HCV-infected patients (right panels). Red dots represent the observed AL-335, ALS-022399, and ALS-022227 plasma concentrations and red dotted lines represent the 5th, 50th, and 95th percentiles of the observed concentrations. The shaded areas represent the 95% CI of the simulated 5th, 50th, and 95th percentiles

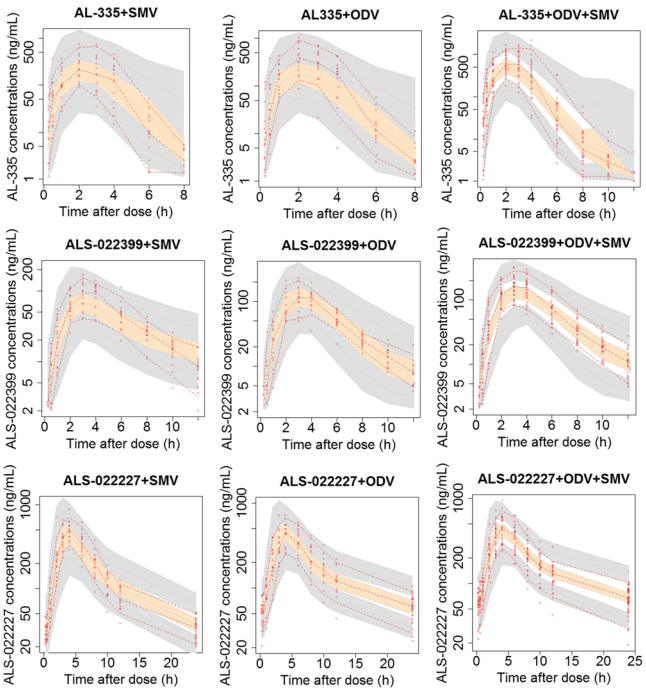

Fig. 6. Visual predictive check of AL-335, ALS-022399, and ALS-022227 in combination with simeprevir (SMV) (left panels), odalasvir (ODV) (middle panels), and ODV + SMV (right panels). Red dots represent the observed AL-335, ALS-022399, and ALS-022227 plasma concentrations and red dotted lines represent the 5th, 50th, and 95th percentiles of the observed concentrations. The shaded areas represent the 95% CI of the simulated 5th, 50th, and 95th percentiles

main metabolites (ALS-022399 and ALS-022227) in healthy and HCV-infected subjects after oral administration of AL-335 alone or in combination with simeprevir and/or odalasvir.

A one-compartment model with a lagged sequential zero-first-order absorption and linear elimination was suitable to describe AL-335 pharmacokinetics. The absorption half-life was determined to be 43 min, after 1.67 h of continuous drug release for absorption in healthy subjects or 2.44 h in HCV-infected subjects. In healthy subjects, a short lag time (≈5 min) was estimated while this parameter was negligible in HCV-infected subjects. This absorption kinetics was adequate to properly characterize the C_{max} and t_{max} which on average (standard deviation (SD)) were 92.0 (35.8) ng/mL and 2.15 (0.97) h, respectively. The typical apparent volume of distribution for central compartment (IIV) was estimated to be 697 L (80.9%). The AL-335 bioavailability in humans has not been determined given the lack of data after intravenous administration. However, preclinical studies in dogs indicated a moderate oral bioavailability (12.5%) (data on file). Assuming a comparable bioavailability in humans, the "real" volume of distribution for AL-335 would be 87 L, a value that exceeds the total body water (35 L) indicating moderate tissue distribution and consistent with the physio-chemical properties of AL-335. Moreover, the plasma protein binding of AL-335 was determined to be 41.3% in humans (data on file).

The apparent clearance (IIV) of AL-335 was determined to be high, 3300 L/h (33.9%) and reflects a fast metabolism, mainly in liver and plasma, with a short half-life (≈8.76 min). Enzymatic conversion in the liver of AL-335 to ALS-022399 occurs via cathepsin A and/or carboxylesterase-1, the latter is expected to be the main enzyme involved in hepatic metabolism of AL-335 (data on file). This fast clearance is in line with values previously determined in preclinical studies but, in this particular analysis, should be interpreted with caution given the number of plasma concentrations below LLOQ that were not included in the modeling. In order to explore the influence of the below LLOQ concentrations on model structure and parameters estimates, the implementation of a M3 method was performed (19) but a successful minimization could not be obtained. The interpretation of the current results does not appear to be jeopardized by the number of plasma concentrations below LLOQ, given the fact that the model is able to describe the time course of ALS-022227 that is indeed the moiety related to the biological activity.

The best model describing ALS-022399 was a two-compartment model with linear elimination. The model was adequate to properly characterize the C_{max} and t_{max} which on

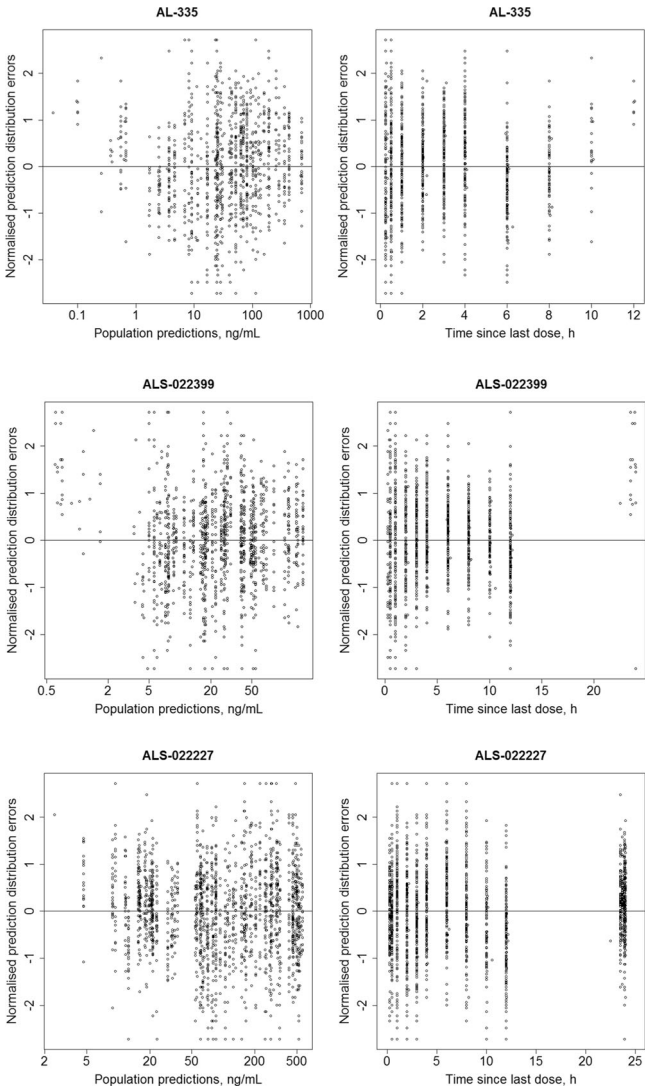

Fig. 7. Normalized prediction distribution errors (NPDE) plots for AL-335, ALS-022399, and ALS-022227

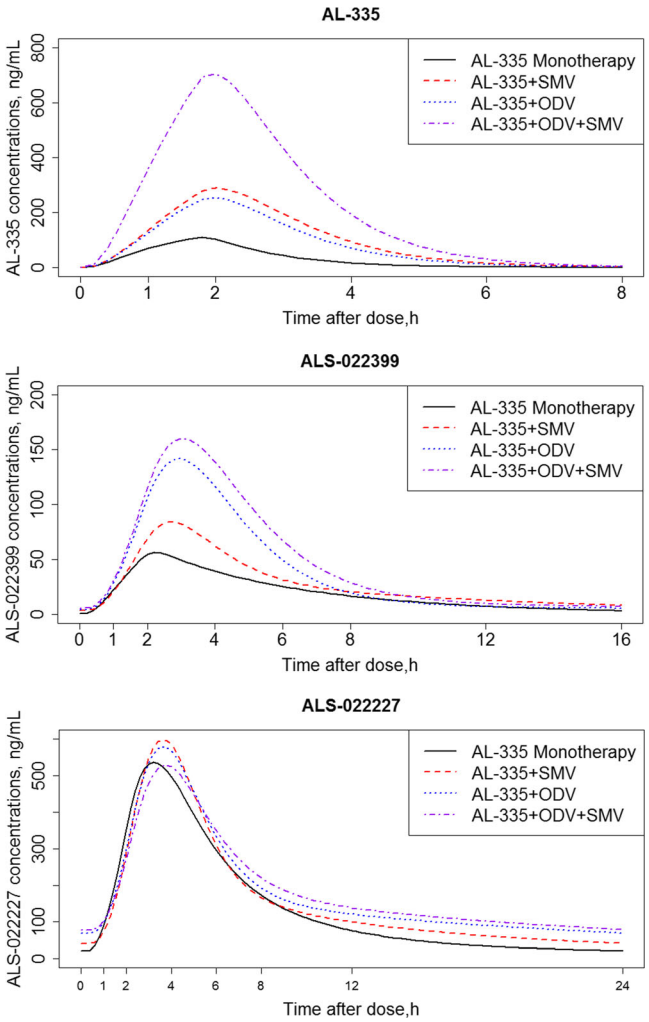

Fig. 8. Deterministic simulations evaluating the effect of simeprevir (SMV) (- - -lines), odalasvir (ODV) (··· lines), or both (·-·-·- lines) on AL-335 (upper panel), ALS-022399 (medium panel), and ALS-022227 (lower panel) plasma concentrations

average (SD) were 51.4 (6.6) ng/mL and 2.83 (0.92) h, respectively. The fraction of AL-335 transformed in ALS-022399 was assumed to be 100%, which was supported by in vitro and preclinical data (not published). The estimate of the steady state volume (V_{ss}) for ALS-022399, 7340 L, clearly exceeded the total body water. The large peripheral volume of distribution, compared to the central volume, suggests a wide non-specific distribution of the compound, which may include the intracellular distribution. In the liver, ALS-022399 is converted to the monophosphate metabolite AL-316 by histidine triad nucleotide binding protein-1 (Hint1) mediated metabolism that is later transformed into ALS-022227, with a fast $t_{1/2\alpha}$ (8.6 min) and a $t_{1/2\beta}$ close to 3.3 h.

A two-compartment model with linear distribution and nonlinear elimination was adequate to capture ALS-022227 plasma concentrations and to properly characterize the C_{max} and t_{max} which on average (SD) were 483.1 (116.7) ng/mL and 3.81 (0.76) h, respectively. The typical value of $V_{ALS-022227}$ (IIV, %) was 76.2 L (78.7%), 21-fold and 43-fold smaller than $V_{ALS-022399}$ and V_{AL-335}, respectively. The V_{ss} for ALS-022227 was determined to be 1057 L. Moreover, ALS-022227 clearance was adequately described using Michaelis-Menten elimination kinetics characterized by a $V_{max,ALS-022227}$ of 84,799 ng/h and a $K_{m,ALS-022227}$ of 450.2 ng/mL. Taking into account the linear collapse of the Michaelis-Menten kinetics when ALS-022227 plasma concentrations were lower than K_m, the linear clearance estimation will be close to 188 L/h, significantly slower than $CL_{ALS-022399}$ and CL_{AL-335}. Together with the lower central volume of distribution, this clearance determined higher plasma concentrations of ALS-022227 compared to ALS-022399 and AL-335, and an elimination half-life of approximately 17 h. AL-335 was mainly recovered in urine as ALS-022227 with 13.5% of the total dose being measurable as ALS-022227, thus suggesting renal excretion of this metabolite (data on file).

The average effect of simeprevir, odalasvir or simeprevir + odalasvir was evaluated as a categorical effect on parameters of the different entities. The model will require further evaluation to assess if the identified effects were dependent on drug concentrations or not, and whether other doses of simeprevir and/or odalasvir would lead to similar interaction effects. AL-335 plasma concentrations were increased when

co-administered with simeprevir or odalasvir and to a more pronounced extent when both odalasvir and simeprevir were co-administered. The co-administration with odalasvir was responsible for a 62.9% decrease in CL_{AL-335} whereas the co-administration of simeprevir was responsible for a 68.8% decrease in CL_{AL-335}. The effect of the simultaneous co-administration of odalasvir and simeprevir was estimated to be less than the sum of the individual effects (86.6% decrease of CL_{AL-335}). The inclusion of the effect of odalasvir, simeprevir, or odalasvir + simeprevir on absorption parameters (ka, D1, bioavailability) did not improve the description of the DDI process. However, the estimation of V_{AL-335} was five times lower in the model including odalasvir + simeprevir effects compared to other models including odalasvir or simeprevir effects or describing monotherapy data. The inclusion of the effect of odalasvir + simeprevir on V_{AL-335} in the model improved the OFV and the model stability; however, the physiological meaning of this effect is largely unknown. Odalasvir has been reported to be a P-glycoprotein inhibitor (10), simeprevir a P-glycoprotein substrate and inhibitor (11) and AL-335 a P-glycoprotein substrate (10). The increase in AL-335 plasma concentrations may be explained by the capacity of odalasvir and simeprevir to inhibit P-glycoprotein transport. The effect on $CL\text{-}AL_{335}$ might not represent the impact on a specific enzyme involved in the transformation of AL-335 to ALS-022399 but might be more representative of a P-glycoprotein inhibition occurring both at intestinal and/or hepatic level. The absence of IV data did not allow to separate CL and F completely, and an effect of co-administered drugs on the apparent clearance of AL-335 (CL/F) could also be partially attributed to an effect on F, making the physiological interpretation of this effect more challenging. The effect of odalasvir + simeprevir on V_{AL-335} could be attributed to a stronger interaction process involving P-glycoprotein at the intestinal level when odalasvir + simeprevir are co-administered, thus leading to an alteration of the scaling factor between doses and drug concentrations (i.e., bioavailability). The absence of intravenous data and the correlation between clearance and disposition trough the relative bioavailability, makes the identification of the underlying physiological process challenging.

ALS-022399 and ALS-022227 plasma concentrations were also modified in the presence of simeprevir and/or odalasvir. The estimated effect of odalasvir + simeprevir over $CL_{ALS-022399}$ (reduced by 60.2%), $Q_{ALS-022399}$ (reduced by 96.1%) and $K_{m,ALS-022227}$ (increased by 55.0%) was also lower than the sum of the individual effects of each co-treatment. This suggests that odalasvir and simeprevir are probably competing to inhibit the transporters or enzymes involved in the drug-drug interaction. An effect of odalasvir on $Q_{ALS-022227}$ was identified. The magnitude of the increase was slightly different between a co-treatment with odalasvir (220% increase) and odalasvir + simeprevir (250% increase). No effect of simeprevir on $Q_{ALS-022227}$ has been shown. However, as simeprevir is increasing odalasvir concentrations (15), it can explain the higher estimated effect for odalasvir + simeprevir compared to odalasvir. As PK parameters were apparent, the effect identified on $Q_{ALS-022399}$ and $Q_{ALS-022227}$ can be confounded with an effect on bioavailability. The increase in ALS-022399 plasma concentrations may be the consequence of the increase in ALS-335, as well as the capacity of odalasvir and simeprevir to inhibit intracellular enzymes involved in the phosphorylation and dephosphorylation of this entity and contributing to it elimination. The slight increase in ALS-022227 plasma concentrations is currently unexplained, as this entity has not been identified to be a substrate of a transporter odalasvir and/or simeprevir could affect.

The population pharmacokinetic model developed could be expanded to account for the following: (1) potential nonlinearities in the pharmacokinetics processes including a broader dose range of AL-335 beyond the 800-mg dose level, (2) potential influence of covariates on pharmacokinetics parameters (was not explored in the current analysis), and (3) potential differences in the magnitude of the interaction process between simeprevir and/or odalasvir with AL-335 in chronic HCV-infected subjects, as the expression of transporters and enzymes can be modified in this population (11).

CONCLUSIONS

An integrated population pharmacokinetic model simultaneously describing the pharmacokinetics of AL-335 and its two main metabolites (ALS-022399 and ALS-022227) in monotherapy, in healthy subjects, and HCV-infected subjects was successfully developed and evaluated. The inclusion of an effect of simeprevir, odalasvir, and odalasvir + simeprevir on AL-335, ALS-022399, and ALS-022227 pharmacokinetics allowed us to describe the magnitude of the interaction in healthy subjects and could be useful to evaluate the impact of simeprevir and/or odalasvir on AL-335 pharmacokinetics in HCV-infected subjects.

ACKNOWLEDGMENTS

The authors thank Eef Hoeben for her comments and support during the analysis. In addition, the authors would like to thank the patients, investigators, and their medical, nursing, and laboratory staff who participated in the clinical trials included in the present study.

COMPLIANCE WITH ETHICAL STANDARDS

Each protocol was reviewed and approved by an institutional review board and written informed consent was obtained from each subject before enrollment in the studies, after being advised of the potential risks and benefits of the study. The studies were conducted in agreement with the Declaration of Helsinki, Good Clinical Practices guidelines, and other applicable regulatory requirements.

Conflict of Interest Matthew W. McClure was an employee of Alios BioPharma Inc., part of the Janssen Pharmaceutical Companies, at the time this study was conducted.

REFERENCES

1. World Health Organization. Fact sheet hepatitis C. July 2017. http://www.who.int/mediacentre/factsheets/fs164/en/. Accessed 26 Sep 2017.

2. Pawlotsky J-M, Chevaliez S, McHutchison JG. The hepatitis C virus life cycle as a target for new antiviral therapies. Gastroenterology. 2007;132(5):1979–98. https://doi.org/10.1053/j.gastro.2007.03.116.
3. World Health Organization. Guidelines for the screening, care and treatment of persons with chronic hepatitis C infection. Updated version April 2016. 2016. http://apps.who.int/iris/bitstream/10665/205035/1/9789241549615_eng.pdf?ua=1. Accessed 18 Sep 2017.
4. Lawitz E, Matusow G, DeJesus E, Yoshida EM, Felizarta F, Ghalib R, *et al.* Simeprevir plus sofosbuvir in patients with chronic hepatitis C virus genotype 1 infection and cirrhosis: a phase 3 study (OPTIMIST-2). Hepatology. 2016;64(2):360–9. https://doi.org/10.1002/hep.28422.
5. Lawitz E, Poordad F, Hyland RH, Wang J, Liu L, Dvory-Sobol H, *et al.* Ledipasvir/sofosbuvir-based treatment of patients with chronic genotype-1 HCV infection and cirrhosis: results from two phase II studies. Antivir Ther. 2016;21(8):679–87. https://doi.org/10.3851/IMP3062.
6. National Center for Biotechnology Information. PubChem Compound Database; CID=118596336, https://pubchem.ncbi.nlm.nih.gov/compound/118596336. Accessed 16 Aug 2018.
7. Tan H, Shaw K, Jekel A, Deval J, Jin Z, Fung A, *et al.* Preclinical characterization of AL-335, a potent uridine based nucleoside polymerase inhibitor for the treatment of chronic hepatitis C. J Hepatol. 2015;62(2):S577–8.
8. Gerber L, Welzel TM, Zeuzem S. New therapeutic strategies in HCV: polymerase inhibitors. Liver Int. 2013;33(1):85–92. https://doi.org/10.1111/liv.12068.
9. OLYSIO® (simeprevir) prescribing-information. 2013. https://www.olysio.com/shared/product/olysio/prescribing-information.pdf. Accessed 18 Sep 2017.
10. Kakuda TN, McClure MW, Westland C, Vuong J, Homery M-C, Poizat G, *et al.* Pharmacokinetics, safety, and tolerability of the 2- and 3-direct-acting antiviral combination of AL-335, odalasvir, and simeprevir in healthy subjects. Pharmacol Res Perspect. 2018;60(3):e00395. https://doi.org/10.1002/prp2.395.
11. Ouwerkerk-Mahadevan S, Snoeys J, Peeters M, Beumont-Mauviel M, Simion A. Drug-drug interactions with the NS3/4A protease inhibitor simeprevir. Clin Pharmacokinet. 2016;55(2):197–208. https://doi.org/10.1007/s40262-015-0314-y.
12. Beal S, Boeckman A, Scheiner L. NONMEM user's guides. San Francisco,CA: University of California at San Francisco. 1988.
13. R Development Core Team 2007. R: A language and environment for statistical computing. R Foundation for Statistical Computing, Vienna, Austria. ISBN 3-900051-07-0, URL http://www.R-project.org.
14. Bertrand J, Laffont CM, Mentré F, Chenel M, Comets E. Development of a complex parent-metabolite joint population pharmacokinetic model. AAPS J. 2011;13(3):390–404. https://doi.org/10.1208/s12248-011-9282-9.
15. Valade E, Hoeben E, Kakuda TN, McClure M, Westland C, Perez Ruixo J, Ackaert O. Population pharmacokinetic modeling of simeprevir – odalasvir interaction in healthy volunteers. 26th Population Approach Group in Europe, June 2017; Budapest, Hungary. https://www.page-meeting.org/default.asp?abstract=7233. Accessed 26 Sep 2017.
16. Brendel K, Comets E, Laffont C, Laveille C, Mentré F. Metrics for external model evaluation with an application to the population pharmacokinetics of gliclazide. Pharm Res. 2006;23(9):2036–49. https://doi.org/10.1007/s11095-006-9067-5.
17. Nguyen TH, Comets E, Mentré F. Extension of NPDE for evaluation of nonlinear mixed effect models in presence of data below the quantification limit with applications to HIV dynamic model. J Pharmacokinet Pharmacodyn. 2012;39(5):499–518. https://doi.org/10.1007/s10928-012-9264-2.
18. Yano Y, Beal SL, Sheiner LB. Evaluating pharmacokinetic/pharmacodynamic models using the posterior predictive check. J Pharmacokinet Pharmacodyn. 2001;28(2):171–92.
19. Ahn JE, Karlsson MO, Dunne A, Ludden TM. Likelihood based approaches to handling data below the quantification limit using NONMEM VI. J Pharmacokinet Pharmacodyn. 2008;35(4):401–21. https://doi.org/10.1007/s10928-008-9094-4.